3/5/98 Post Print Document
This paper was published as Pai, Y. C., Patton, J., L., "Center of mass velocity-position predictions for balance control" *Journal of Biomechanics*, 30(4):347-354, 1997. The following copy reflects the erratum submitted later and final revisions.

CENTER OF MASS VELOCITY-POSITION PREDICTIONS FOR BALANCE CONTROL

Yi-Chung Pai[1] and James Patton[2]

[1]Programs in Physical Therapy,
Northwestern University Medical School, Chicago, IL 60611

[2]Biomedical Engineering Graduate Program,
Northwestern University, Evanston, IL 60208 (j-patton@nwu.edu)

Running title: *Dynamic balance control*

Keywords: Movement termination, Human stance, Initiation of fall, Slipping, Movement constraints, Predicted ability, Simulation model, Optimization

Correspondence address: Yi-Chung Pai, Ph.D.
Programs in Physical Therapy,
Northwestern University Medical School
645 N. Michigan Ave., Suite 1100
Chicago, IL 60611, USA
Ph: (312) 908-8273
Fax: (312) 908-0741
e-Mail: c-pai@ nwu.edu

Abstract

The purposes of this analysis were to predict the feasible movements during which balance can be maintained, based on environmental (contact force), anatomical (foot geometry), and physiological (muscle strength) constraints, and to identify the role of each constraint in limiting movement. An inverted pendulum model with a foot segment was used with an optimization algorithm to determine the set of feasible center of mass (CM) velocity-position combinations for movement termination. The upper boundary of the resulting feasible region ran from a velocity of 1.1 s^{-1} (normalized to body height) at 2.4 foot lengths behind the heel, to 0.45 s^{-1} over the heel, to zero over the toe, and the lower boundary from a velocity of 0.9 s^{-1} at 2.7 foot lengths behind the heel, to zero over the heel. Forward falls would be initiated if states exceeded the upper boundary, and backward falls would be initiated if the states fell below the lower boundary. Under normal conditions, the constraint on the size of the base of support (BOS) determined the upper and lower boundaries of the feasible region. However, friction and strength *did* limit the feasible region when friction levels were less than 0.82, when dorsiflexion was reduced more than 51%, or when plantar flexion strength was reduced more than 35%. These findings expand the long-held concept that balance is based on CM *position* limits (*i.e.*, the horizontal CM position has to be confined within the BOS to guarantee stable standing) to a concept based on CM *velocity-position* limits.

Introduction

The control of balance is an essential component of human movements. A single, quantitative criterion for assessing a person's ability to control balance, however, is often difficult to establish, primarily because there are many feasible movements to choose from which accomplish the same task. One strategy for resolving this issue is to quantify various constraints that a person has to negotiate in the performance of a task, and then to use these constraints to identify the *range of feasible movements* in which the control of balance can be maintained.

Previous studies have investigated feasible ranges in acceleration, torque, or manual force application spaces under various constraints necessary for a person to maintain standing balance by keeping their feet stationary (Levine *et al.*, 1983; Nashner *et al.,* 1989, Gordon, 1990; Yang *et al.*, 1990; Kuo and Zajac, 1993; Kerk *et al*., 1994; Kuo, 1995). For instance, Gordon (1990) introduced the idea that certain physical constraints (*i.e.*, muscle strength, the need for the foot to remain on the floor, etc.) can be mapped into the acceleration space. In his work, a model of the foot segment was used to introduce constraints on the dynamics of a three-joint planar model of standing. A feature lacking in these studies was an understanding of how the range of feasible movements could be influenced by the interaction of several task constraints. For example, the interplay between velocity and position has never been examined in balance dynamics, presumably because velocities are considered low in nearly static standing.

Traditionally, the feasible movements for the control of balance are described in a single dimensional space related to the horizontal position of the body center of mass (CM): A person has to confine projection of the CM within the base of support (BOS)[1] in order for the body to remain balanced while standing (Borelli, 1680; Dyson, 1977; Patla *et al*., 1990; Kuo, 1995). This condition alone, however, is not sufficient to guarantee that standing posture *will* be sustained. Only recently, has it been proposed that the horizontal velocity of the CM should also be considered in describing the feasible movements for the control of balance (Pai *et al*., 1992), because it governs the destiny of the horizontal position of the CM over the BOS. Standing will not be maintained when a sufficiently large horizontal velocity exists, even though the horizontal CM is currently located inside the BOS. Conversely, it is possible for the CM to initially be located outside the BOS, as in movement termination, and still be able to achieve upright standing (without falling or resorting to taking a step), provided that sufficient horizontal CM velocity is directed toward the BOS (Pai *et al*., 1994). Thus, besides the horizontal location of the CM with respect to the BOS, the magnitude and the direction (*i.e.*, toward, not away from, the BOS) of its corresponding velocity may also provide critical information pertaining to one's ability to control balance.

The combination of the above two concepts (using constraints to predict a person's feasible movements and using CM velocity-position interactions to understand

[1] In standing, the base of support is the roughly trapezoidal contact area between the feet and the floor, in which the resultant ground reaction force from the floor can be applied to the plantar surface of the feet. In this analysis, it becomes a region within the anteroposterior length of the foot where the center of pressure may actually travel.

dynamic balance) has at least two practical implications. To date, the clinical assessments in physical rehabilitation are mostly centered on identifying regional limitations of a joint or a segment (*e.g.*, joint range of motion assessment, muscle strength assessment, sensation assessment). Nevertheless, such assessments rarely provide clinicians with a global description of a patient's capability to perform daily tasks. Linking regional constraints to global motion can offer the basis for using the results of joint assessments to predict the feasible CM movements that a patient can perform, so that the functional goals for therapeutic intervention can more likely be quantified.

Furthermore, in the past few decades, substantial effort has been made to understand and to assess a person's ability to maintain a standing posture under both unperturbed and perturbed conditions (Hellebrandt *et al.*, 1938; Murray *et al.*, 1975; Sheldon, 1963; Nashner, 1976; Dietz *et al.*, 1985). Clinical observations indicate, however, that falls most frequently occur during activities involving larger displacements of the CM, such as walking, stepping up or down, or standing up (Tinetti *et al.*, 1988). The assessment of one's ability to control balance during small *and* large CM velocities and changes in positions (vs. just small changes in position, as in standing) would be appropriate and valuable in the prevention of falls.

Consequently, this analysis presents a modeling approach that addresses two questions: (1) Which velocity-position combinations can a person tolerate and still regain balance without initiating a fall? (Specifically, which velocities are insufficient, initiating a backward fall, or excessive, initiating a forward fall?) and (2) What is the role of each constraint in altering the person's feasible movements? The model identified the constraints which dictate the dynamic limits of balance under normal conditions, and also identified the conditions under which other constraints become restricting. In this initial analysis , the focus is limited to mechanical constraints, to a simple pendulum model, and to anterior movements, although the methodology can be expanded to neural constraints, to more complex models, and to posterior and lateral movements.

Methods

A simple two-segment sagittal model included a foot segment that provides a BOS on the floor, and an inverted pendulum (Figure 1). Foot position was assumed to be bilaterally symmetrical and stationary. Typical male proportions (Table 1) were used to determine anatomical parameters (Winter, 1990). Based on this model, the equations of motion were formulated (Appendix).

Table 1: *Summary of the anthropometric scaling scheme used*

Body height	**H= 1.78 m**
Body mass	**mass= 80 kg**
Foot mass	m_f= 2 X 0.0145 X mass
Pendulum mass	m = mass - m_f
Pendulum length	l= 0.575 X H
Foot length	l_f= 0.152 X H
Horizontal ankle-to-heel	a= 0.19 X l_f
Vertical ankle height	b= 0.039 X H
Horizontal ankle-to-CM of	c= 0.5 X l_f - a

The objective of the optimization was to identify the boundaries of all possible velocity-position combinations which may satisfy the task conditions*:* The mass must arrive at a position over the BOS as the velocity vanishes, while the feet remain stationary. Thus, at any given CM position, two *boundary velocities* were defined, beyond which the task could not be accomplished without foot motion:

1. The *largest tolerable velocities* that still can be reduced to zero before the CM exceeds the anterior limit of the BOS.
2. The *smallest necessary velocities* that still allow the CM to reach the posterior limit of the BOS.

Because the foot was not rigidly attached to the floor, the model's ability to transmit forces from the floor to the BOS was limited by three constraints:

1. Gravity constraint: The net vertical ground reaction force, F_{gy}, must be positive:
$$F_{gy} \geq 0 \qquad (1)$$
2. Friction constraint: The horizontal ground reaction force, F_{gx}, must not exceed the slip threshold dictated by the coefficient of friction, m:
$$|F_{gx}| < mF_{gy} \qquad (2)$$
3. Center of pressure (COP) constraint: The COP must reside within the length of the BOS, lf :
$$0 < COP < l_f \qquad (3)$$

Each of these inequality equations was then algebraically related to the dynamics of the pendulum (Appendix), and expressed in terms of the angular position, Θ , angular velocity, $\dot{\Theta}$, and resultant ankle torques, τ, resulting in boundaries in the *state-torque space*:

$$\left\{\begin{array}{l} t_{gravity} > f_g(\Theta,\dot{\Theta}) \\ t_{slip\_anterior} > f_a(\Theta,\dot{\Theta}) \\ t_{slip\_posterior} < f_p(\Theta,\dot{\Theta}) \\ t_{COP\_heel} < f_h(\Theta,\dot{\Theta}) \\ t_{COP\_toe} > f_t(\Theta,\dot{\Theta}) \end{array}\right\} \qquad (4)$$

In addition to these constraints, the resultant ankle torques, τ, were physiologically constrained to a range of values under maximum muscle strength:

$$(t)_{maximum\_plantarflexion} \leq t \leq (t)_{maximum\_dorsiflexion} \qquad (5)$$

The maximum values for the τ were assumed to be dependent on joint position, and were taken from a musculoskeletal model (see Figure 6, page 761 in Delp et al., 1990). This Hill-based model considers the force-length properties of muscles crossing the ankle, the lines of action of all musculotendonous elements, and sums their effect to estimate the maximum dorsiflexion and plantar flexion torques.

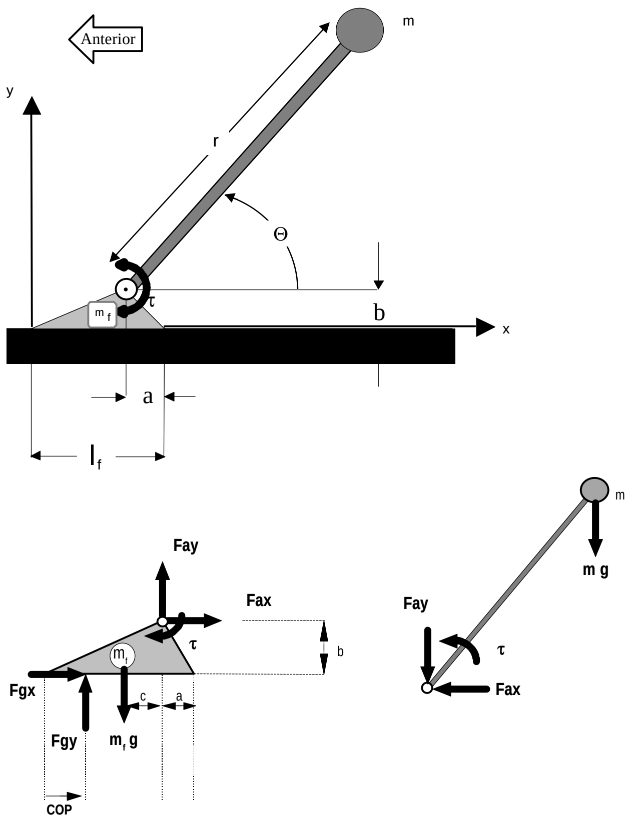

Figure 1. *Pendulum and foot model with free body diagrams for the segments.*

A switching state feedback controller (Figure 2, solid lines) considered each constraint (Equations 4 and 5), and determined the maximum and minimum feasible torque necessary to keep the feet stationary (Figure 2, solid lines). Using this controller, two optimal CM velocity-position trajectories were obtained iteratively by adjusting the initial states (Figure 2, broken lines). These optimal trajectories either maximized or minimized the initial velocity that still allowed the task to be completed successfully (*i.e.*, the CM arrived precisely above the anterior or posterior limit of the BOS as the velocity vanished, while the feet remained stationary). The trajectory with the "fastest" initial velocity at the most posterior initial position was used to define the fall-forward boundary, and the trajectory with the "slowest" initial velocity at the most posterior initial position was used to define the fall-backward boundary. A fifth order Runge-Kutta method with a fourth order step-size control (MATLAB, Math Works, Inc., Natick, Mass, U.S.A.) was used to integrate the equation of motion (Equation A1, Appendix).

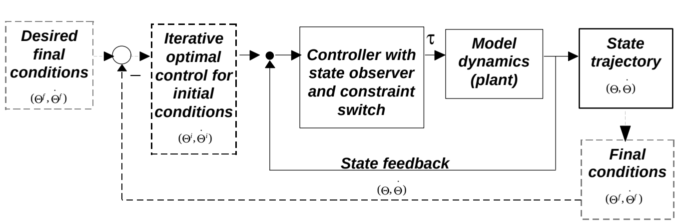

Figure 2. *Optimization scheme. A switching state feedback controller (using the bounding surfaces to determine the maximum and minimum feasible torque for a given state [solid lines]), obtained two optimal center of mass velocity-position trajectories iteratively by adjusting the initial states (broken lines).*

Additional analyses were conducted to calculate the threshold values where key parameters started to affect the feasible region, and to identify the effects of extreme conditions. Consequently, friction was reduced iteratively to an extreme value of $\mu = 0.05$ to simulate slippery conditions (oil on metal, *cf.* Chaffin *et al.*, 1992; Lloyd and Stevenson 1992). Similarly, strength was reduced 59% to simulate the weakness in an elderly group (elderly mean minus one standard deviation in Gerdle and Fugl-Meyer, 1985), and because the COP range observed in elderly subjects during functional activities can be much smaller than the full foot length, the range of the BOS was reduced 55% (an extreme case in Lee and Deming, 1988).

Results

The upper boundary of the resulting feasible region ran from a velocity of 1.1 s^{-1} (normalized to body height) at 2.4 foot lengths behind the heel, to 0.45 s^{-1} over the heel, to zero over the toe, and the lower boundary ran from a velocity of 0.9 s^{-1} at 2.7 foot lengths behind the heel, to zero over the heel (gray area, Figure 3). Forward falls would be initiated if states exceeded the upper boundary, and backward falls would be initiated if the states fell below the lower boundary.

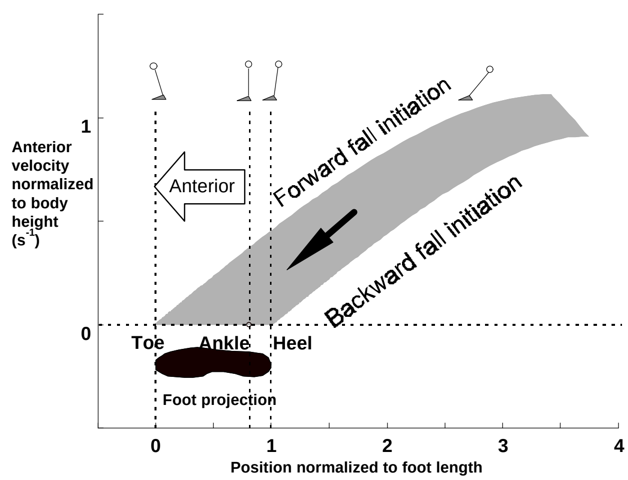

Figure 3. *Feasible horizontal center of mass velocity-position region (shaded diagonal band) for terminating anterior movement of a simple pendulum connected to a stationary base of support. Forward falls would be initiated if states exceeded the upper boundary, while backward falls would be initiated if states dropped below the lower boundary. The initiation of a fall was also defined in this analysis as any dynamic condition that causes the feet to move. Velocities and positions were normalized by body height and foot length, respectively (toe is zero and heel is 1). The bold arrow indicates the direction a trajectory would travel in terminating movement.*

Under normal conditions, the COP_{toe} constraint determined the upper boundary of the feasible region (Figure 4, lower surface and trajectory), while the COP_{heel} constraint determined the lower boundary (Figure 4, upper surface and trajectory), and the gravity constraint (Equation 1) determined the posterior boundary of the feasible region (Figure 3, upper right edge of the gray area).

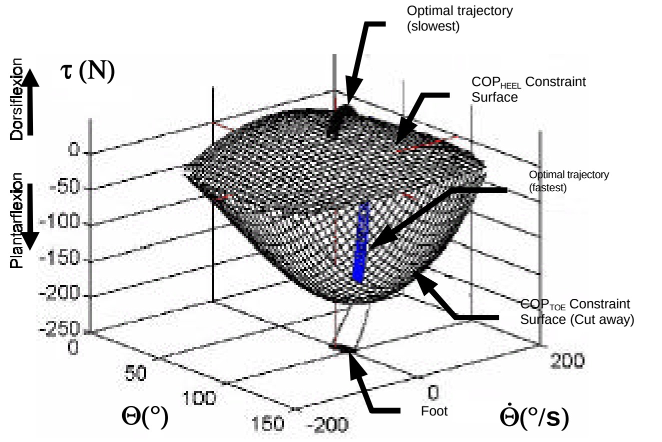

Figure 4. Innermost bounding constraint surfaces in the state-torque space, the optimal trajectories, and their projection onto the velocity-position phase plane (bottom). Dark bold lines on bounding constraint surfaces represent the two optimal trajectories (the "fastest" and the "slowest"), both of which begin at points at the back of the surface (out of view) and come toward the viewer. A representation of the foot in black shade is also drawn to show relative position on the phase plane.

Normal friction and strength constraints did not limit the feasible region unless friction levels were less than 0.82, dorsiflexion strength was reduced more than 51%, and plantar flexion strength was reduced more than 35%. Extreme alterations in friction and strength beyond these threshold values further reduced the feasible region (Figure 5).

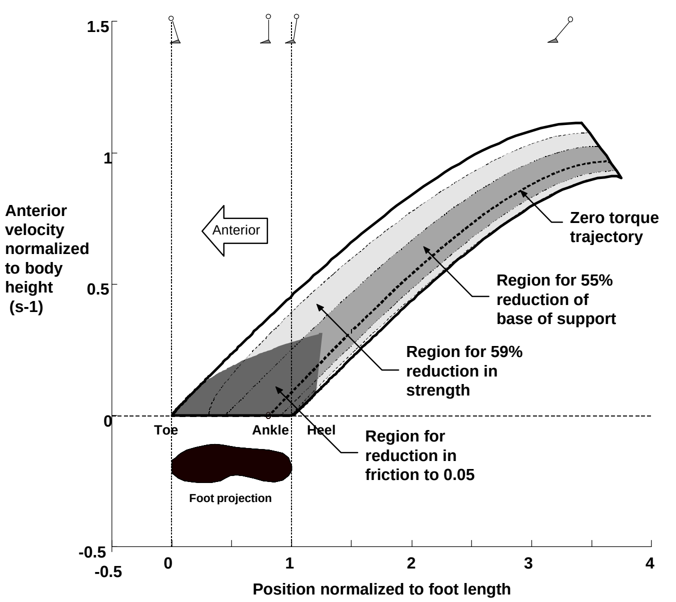

Figure 5. Normal feasible region (same diagonal band as in Figure 3 is enclosed by thick solid lines) altered under reduced friction, strength, and base of support conditions: Friction was reduced to m =0.05 to simulate slippery conditions (dark shaded area); strength was reduced 59% to simulate the weakness in an elderly group (light shaded area); functional base of support was reduced 55% to simulate an extreme case in the elderly (intermediately shaded area). The unique trajectory that requires zero resultant torque is also shown (thick broken line).

Discussion

The analysis presented here demonstrates that an individual's ability to terminate anterior movement can be estimated with a computer model when the anatomical, physiological, and environmental constraints are considered. The diagonal shape of the feasible region (Figure 3) indicates the interaction between the CM velocity and its position, *i.e.*, a person can tolerate higher anterior velocities at more posterior CM positions without initiating a fall.

The computer model used to derive these results was based on several simplifying assumptions, which therefore might limit its predictive capacity. For example, a single segment was assumed above the ankle joint. Movement termination was assumed to occur in the sagittal plane. It was assumed that to avoid an impending fall, a person may resort to instantaneous exertion of muscle strength at its maximum value (although for normal conditions, the model did not utilize maximum strength due to other constraints being more restrictive). The model also assumed that strength is dependent on joint position alone, and neglected the possibility that heel and toe rise could occur without initiating a fall. Overall, the effects of multisegmental interactions (*i.e.*, the contributions of joints other than the ankle), of three-dimensional movement, of heel and toe rise, of joint velocity on strength limits, of rate-limits on muscle activation (*cf*. Zajac, 1989), and of other neurological constraints (*cf*., Nashner *et. al*., 1989) may influence the actual values of the predicted feasible region, and should be taken into consideration in future work. Two key concepts applied in this analysis -- the use of regional constraints to predict one's global ability to perform a functional task and the use of CM velocity-position interaction to understand dynamic balance -- are applicable to more complex and perhaps more insightful models than this endeavor.

Nevertheless, in spite of these limitations, the model predictions were consistent with previously published experimental data and trajectories derived from studies on gait, sit-to-stand (STS), STS followed by a volitional forward fall, and balance recovery from a horizontal bimanual pull. When the second foot touches the ground at the end of the final step in gait termination (Jian et al., 1993), the horizontal CM velocity-position combination was located well within the predicted feasible region (Figure 6, open square). Also as predicted, the ensemble average of the horizontal CM trajectories for both slow and fast STS (Pai and Rogers, 1990) started in the backward fall region E, but traveled out of it and into the feasible region D (Figure 6, solid lines) before subjects lost contact with the chair. In fact, the fast STS trajectory was located outside of the BOS when subjects lost contact with the chair (indicated by ⊗ in region D, Figure 6), yet was well within the feasible region. The velocity for the STS followed by a volitional forward fall (Pai and Lee, 1994) actually exceeded the feasible region before the instant of losing contact with the chair (indicated by circled X in region A, Figure 6). Finally, for the pendulum-like standing pull task (Michaels et. al., 1993), the horizontal CM velocity-position trajectory during balance recovery after releasing from the pull began outside of the BOS but well within the feasible region (short broken line, Figure 6).

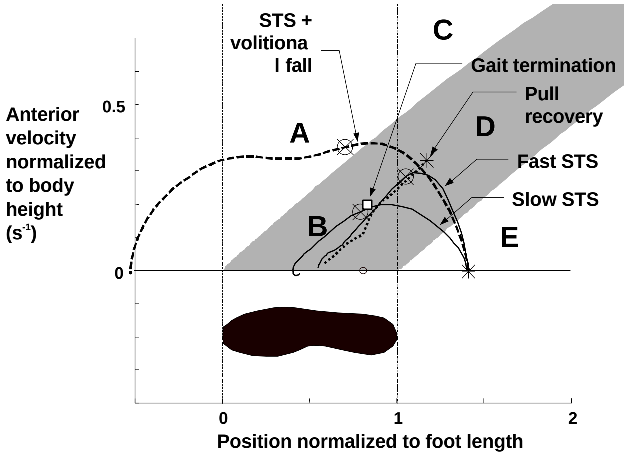

*Figure 6. Comparisons between the predicted velocity-position feasible region (a portion of the light gray diagonal band in Figure 3) and experimental data derived from: (1) gait (open square represents data taken from the time when the second foot touches the ground at the end of the final step in gait termination, Jian et al., 1993); (2) sit-to-stand in slow and fast speeds (trajectories with thin solid lines labeled as "Slow STS" and "Fast STS", Pai and Rogers, 1990); (3) STS followed by a forward fall (trajectory with long broken line labeled as "STS+fall", Pai and Lee, 1994); and (4) balance recovery after releasing from the pull (trajectory with short broken line, labeled as "Pull", Michaels et al., 1993). Both forward fall region A (above shaded area, between toe and heel) and feasible region B (shaded area, between toe and heel) are located inside the base of support, while the forward fall region C (above shaded area, beind heel), feasible region D (shaded area, behind heel), and backward fall region E (below shaded area, beind heel), are behind the base of support. Ä corresponds to the instant of losing contact with the chair in STS. * indicates the beginning of each movement.*

The finding that normal strength limits did not play a restricting role was also consistent with previous work. Schultz and associates (1992) found that during STS, peak ankle torques were very similar in both young and elderly subjects (including those "unable" elderly who needed the assistance of their hands to rise from a chair), and were well below their reported maximum voluntary joint torques. Normal values of resultant ankle torques also did not play a restricting role in balance recovery mechanisms in model simulation of the standing human (Kuo and Zajac, 1993).

Furthermore, the findings of the present analysis are in qualitative agreement with recent observations on perturbed standing and subsequent stepping responses. Carhart and Yamaguchi observed that the faster and the further anterior the horizontal CM was moving after a perturbation, the more likely the person was to take a step (Carhart and Yamaguchi, 1995). This is consistent with the present analysis, which predicts that the feasible velocities become progressively reduced as the CM moves more anteriorly.

The final objective of a protective response after a perturbation (such as in stepping) is still to reduce the total body velocity, as in movement termination. Do and associates (1982) experimentally determined that the greater the perturbation, the greater the stepping velocity, and the greater the stepping length (a more anteriorly placed BOS). By stepping forward, a person effectively shifts the BOS in the anterior direction, presumably leading to an anterior shift in the upper boundary of the feasible region, and making it possible to terminate movement without taking any further steps.

Finally, the findings of this analysis may shed light on the understanding of the likelihood of taking a step when standing is perturbed (McIlroy and Maki, 1995). If the horizontal CM velocity-position combination is located in the fall regions (A, C or E, Figure 6), the model predicts that the person will have *no option* but to step or fall. On the other hand, the present model predicts that if the horizontal CM velocity-position trajectory is located inside the feasible region after a perturbation, the person still has the option of choosing a stepping response. This prediction makes no assertion about steps that might be initiated from the feasible region inside the BOS, as previous studies have speculated (McIlroy and Maki, 1993). Unfortunately, published reports have mostly concentrated on stepping frequency as a function of perturbation magnitude (McIlroy and Maki, 1993; Carhart and Yamaguchi, 1995), and no corresponding CM velocity-position trajectories have been found to verify the model predictions.

In summary, the traditional view that horizontal CM positions must reside inside the BOS to guarantee maintenance of balance in standing (Borelli, 1680; Dyson, 1977; Patla *et al*., 1990; Kuo, 1995) does not sufficiently define the feasible region for movement termination. This analysis has demonstrated that it is also critical to take into account the horizontal velocity of the CM, and has predicted the feasible region for successful movement termination to be a diagonal band in the horizontal CM velocity-position phase plane, located both inside *and* outside of the BOS. The basic conceptual framework demonstrated in this analysis might be applied to the study of segmental interactions in more complex movements, and might provide guidance for the evaluation of balance dysfunction, which, to date, has mostly been identified with the traditional view of balance control (O'Sullivan, 1994).

Acknowledgments: Supported by research grants from the Arthritis Foundation. The authors thank Julie W. Steege and Kay Clifford for their editing assistance, and Wynne A. Lee for the sharing of computer resources provided by NSF IBN-9319601.

APPENDIX: Model equations and constraints

A rigid body model of an inverted pendulum with a triangular base of support (the feet) was assumed (Figure 1). The equations of motion used were:

$$t = mr^2\ddot{\Theta} + mgr\cos\Theta \quad \text{(A1)}$$

$$F_{ax} = mr(\ddot{\Theta}\sin\Theta + \dot{\Theta}^2\cos\Theta) \quad \text{(A2)}$$

$$F_{ay} = mr(-\ddot{\Theta}\cos\Theta + \dot{\Theta}^2\sin\Theta) - mg \quad \text{(A3)}$$

$$COP = l_f - \left[\frac{bF_{gx} - t + cm_f g}{F_{gy}} + a\right] \quad \text{(A4)}$$

$$F_{gx} = -F_{ax} \quad \text{(A5)}$$

$$F_{gy} = m_f g - F_{ay}. \quad \text{(A6)}$$

where F_{gx} and F_{gy} were horizontal and vertical components of the ground reaction force; F_{ax} and F_{ay} were the resultant joint force components; m_f , l_f , *a*, *b*, *c*, and *COP* were the foot mass, the length of the BOS, the distance between the ankle and the heel, ankle height, the distance between the CM of the foot and the ankle, and the distance between the COP and the toe; m, r, Θ, $\dot{\Theta}$, $\ddot{\Theta}$, and τ were mass, length, angular position, velocity, acceleration of the pendulum, and ankle torque.

Each of the BOS constraint inequalities (Equations 1 to 3) can be expressed as a boundary by taking its equation form and expressing it in terms of a relationship between the states (Θ and $\dot{\Theta}$) and the torques. For example, the COP constraint (Equation 3) combined with (A4), substituting (A1) through (A3), resulted in:

$$0 < l_f - \left[\frac{-\frac{bt}{r}\sin\Theta + bmg\cos\Theta\sin\Theta - bmr\dot{\Theta}^2\cos\Theta - \boldsymbol{t} + cm_f g}{\frac{t}{r}\cos\Theta - mg\cos^2\Theta - mr\dot{\Theta}^2\sin\Theta + (m_f + m)g} + a \right] < l_f \qquad \text{(A7)}$$

The torques were then related to the states of the pendulum:

$$\begin{aligned} \boldsymbol{t}_{cop\_toe} = \{ & [b\sin\Theta + (l_f - a)\cos\Theta] mg\cos\Theta + \\ & [(l_f - a)\sin\Theta - b\cos\Theta] mr\dot{\Theta}^2\cos\Theta_y - \\ & (l_f - a)(m_f + m)g + cm_f g\} / \{\tfrac{(l_f - a)}{r}\cos\Theta + \tfrac{(l_f - a)}{r}\sin\Theta + 1\} \end{aligned} \qquad \text{(A8)}$$

$$\begin{aligned} \boldsymbol{t}_{cop\_heel} = \{ & [b\sin\Theta + a\cos\Theta] mg\cos\Theta + \\ & [a\sin\Theta - b\cos\Theta] mr\dot{\Theta}^2\cos\Theta - \\ & a(m_f + m)g + cm_f g\} / \{\tfrac{a}{r}\cos\Theta + \tfrac{a}{r}\sin\Theta + 1\} \end{aligned} \qquad \text{(A9)}$$

For the gravity constraint, Equation (1) was combined with Equations (A3) and (A6), and resulted in:

$$\boldsymbol{t}_{gravity} = mgr\cos\Theta + mr^2\dot{\Theta}^2\tan\Theta - \frac{(m_f + m)g}{\cos\Theta} \qquad \text{(A10)}$$

Similarly, combining Equations (A1), (A3), (A5) and (A6) with Equation (2) gave the *friction constraint*:

$$\begin{aligned} \boldsymbol{t}_{friction\_anterior} = [& (\sin\Theta + m\cos\Theta) mgr\cos\Theta + \\ & (\sin\Theta - m\cos\Theta) mr^2\dot{\Theta}^2 - \\ & mrg(m_f + m)] / [m\cos\Theta - \sin\Theta] \end{aligned} \qquad \text{(A11)}$$

$$\begin{aligned} \boldsymbol{t}_{friction\_posterior} = [& (\sin\Theta - m\cos\Theta) mgr\cos\Theta + \\ & (\sin\Theta + m\cos\Theta) mr^2\dot{\Theta}^2 + \\ & mrg(m_f + m)] / [-m\cos\Theta - \sin\Theta] \end{aligned} \qquad \text{(A12)}$$

References

Borelli, G. A. (1680) *De Motu Animalium* (Translated by Maquet, P., 1989). Spinger Verlag, Berlin.

Carhart, M. R. and Yamaguchi, G. T. (1995) The motor control of stepping response to postural perturbations. *Conf. Proc. 19th Ann. Mtg. ASB* p 57.

Chaffin, D. B., Woldstad, J. C. and Trujillo, A. (1992) Floor/shoe slip resistance measurement. *Am. Ind. Hyg. Assoc. J.* **53**, 283-289.

Delp, S., Delp, S. L., Loan, J. P., Hoy, M. G. and Zajac, F.E. (1990) Interactive graphics-based model of the lower extremity to study orthopaedic surgical procedures. *IEEE Trans. Biomed. Eng.* **37**, 757-767.

Dietz, V. Quintern, J., Berger, W. and Schenck, E. (1985) Cerebral potentials and leg EMG responses associated with stance perturbations. *Exp. Brain Res.* **57,** 348-354.

Do, M. C., Breniere, Y. and Brenguier, P. (1982) A biomechanical analysis of balance recovery during the fall forward. *J. Biomechanics* **15,** 933-939.

Dyson, G. H. G. (1977) *The Mechanics of Athletics*. Holmes & Meier Publishers, New York.

Gordon, M. E. (1990) An analysis of the biomechanics and muscular synergies of human standing. Ph.D. Dissertation, Stanford University, Stanford, CA.

Hellebrandt, F.A., Tepper, R.H., Braun, G. L. and Elliott, M. C. (1938) The location of the cardinal anatomical orientation planes passing through the center of weight in young adult women. *Am. J. Physiol.* **121,** 465-470.

Gerdle, B., A. R. Fugl-Meyer (1985) Mechanical Output and iEMG of Isokinetic Plantar Flexion in 40-64-year-old Subjects. *Acta Physiol. Scand*. **124**:201-211.

Jian, Y., Winter, D. A., Ishac, M. G. and Gilchrist, L. (1993) Trajectory of the body COG and COP during initiation and termination of gait. *Gait & Posture* **1,** 9-22.

Kerk, C. J., Chaffin, D. B., Page, G. B. and Hughes, R. E. (1994) A comprehensive biomechanical model using strength, stability, and COF constraints to predict hand force exertion capability under sagittally symmetric static conditions. *IIE Trans.* **26,** 57-67.

Kuo, A. D. and Zajac F. E. (1993) Biomechanical analysis of muscle strength as a limiting factor in standing posture. *J Biomechanics* **26,** 137-150.

Kuo, A. D. (1995) An optimal control model for analyzing human postural balance. *IEEE Trans. Biomed. Eng.* **42,** 87-101.

Lee, W. A. and Deming, L. R. (1988) Age-related changes in the size of the effective support base during standing. *Phys. Ther.* **68,** 859.

Levine, S., Zajac, F. E., Belzer, M. R., and Zomlefer, M. R. (1983) Ankle controls that produce a maximal vertical jump when others are locked. *IEEE Transactions on Automatic Control.* **AC-28**:1008-1016.

Lloyd, D. G. and Stevenson, M. G. (1992) An investigation of floor surface profile characteristics that will reduce the incidence of slips and falls. *Mech. Eng.* **17,** 99-105.

McIlroy, W. E. and Maki, B. E. (1993) Task constraints on foot movement and the incidence of compensatory stepping following perturbation of upright stance. *Brain Res.* **616,** 30-38.

McIlroy, W. E. and Maki, B. E. (1995) Adaptive changes to compensatory stepping responses. *Gait & Posture* **3,** 43-50.

Michaels, C. F., Lee, W. A. and Pai Y.-C. (1993) The organization of multisegmental pulls made by standing humans: I. Near-maximal pulls. *J. Motor Behav.* **25,** 107-124.

Murray, M.P., Seineg, A. A. and Sepic, S. B. (1975) Normal postural stability and steadiness: quantitative assessment. *J. B. J. S.* **57-A,** 510-516.

Nashner, L. M. (1976) Adapting reflexes controlling the human posture. *Exp. Brain Res.* **26,** 59-72.

Nashner, L.M., Shupert, C. L., Horak, F. B., and Black, F. O. (1989) Organization of posture controls: An analysis of sensory and mechanical constraints. *Progress in Brain Research*. **80**:411-418.

O'Sullivan, S. B. (1994) Motor control assessment. In *Physical Rehabilitation Assessment and Treatment* (Edited by O'Sullivan, S. B. and Schmitz, T.J.). pp 111-131, third edition, F.A. Davis, Philadelphia.

Pai, Y.-C. and Rogers, M. W. (1990) Control of body mass transfer as a function of speed of ascent in sit-to-stand. *Med. Sci. Sports Exer.* **22,** 378-384.

Pai, Y.-C., Naughton, B. J. and Chang, R. W. (1992) Control of dynamic transfer during sit-to-stand among young and elderly individuals. In *Posture and Gait: Control Mechanisms* (Edited by Woollacott, M. and Horak, F.), **Vol 2,** 301-304. University of Oregon, Eugene, OR.

Pai, Y.-C. and Lee, W. A. (1994) Effect of a terminal constraint on control of balance during sit-to-stand. *J. Motor Behav.* **26,** 247-256.

Pai, Y.-C., Naughton, B. J., Chang, R. W. and Rogers, M. W. (1994) Control of body center of mass momentum during sit-to-stand among young and elderly adults. *Gait & Posture* **2,** 109-116.

Patla, A., Frank, J. and Winter, D. (1990) Assessment of balance control in the elderly: Major issues. *Physiother. Can.* **42,** 89-97.

Schultz, A. B., Alexander, N. B. and Ashton-Miller, J. A. (1992) Biomechanical analyses of rising from a chair. *J. Biomechanics* **25,** 1383-1391.

Sheldon, J. H. (1963) The effect of age on the control of sway. *Gerontol. Clin.* **5,** 129-138.

Tinetti, M.E., Speechley, M. and Ginter, S. F. (1988) Risk factors for falls among elderly persons living in the community. *N. Engl. J. Med.* **319,** 1701-1707.

Winter, D. A. (1990) *Biomechanics and Motor Control of Human Movement* John Wiley and Sons, Inc., NY. 2nd ed.

Yang, J. F., Winter, D. A. and Wells, R.P. (1990) Postural dynamics in the standing human. *Biol. Cybern.* **62,** 309-320.

Zajac, F. E. (1989) Muscle and tendon: Properties, models, scaling, and application to biomechanics and motor control. *CRC Crit. Rev. Bioeng.* **17,** 359-411.

ERRATUM

Center of Mass Position-Velocity Predictions for balance control

Yi-Chung Pai and James Patton

In the above article published in the *Journal of Biomechanics*, **30**(4):347-354, (1997), several typographical errors appeared in the equations. These errors only appeared in the final presentation of the equations, therefore did not affect the results. The correct equations are:

$$\begin{aligned} t_{cop\_toe} = \{[&b\sin\Theta + \\ &(l_f - a)\cos\Theta]mg\cos\Theta + \\ &[(l_f - a)\sin\Theta - \\ &b\cos\Theta]mr\dot{\Theta}^2 - \\ &(l_f - a)(m_f + m)g + cm_f g\}/ \\ &\{1 + \tfrac{(l_f - a)}{r}\cos\Theta + \tfrac{b}{r}\sin\Theta\} \end{aligned} \tag{A8}$$

$$\begin{aligned} t_{cop\_heel} = \{[&b\sin\Theta - a\cos\Theta]mg\cos\Theta - \\ &[a\sin\Theta + b\cos\Theta]mr\dot{\Theta}^2 + \\ &a(m_f + m)g + cm_f g\}/ \\ &\{1 - \tfrac{a}{r}\cos\Theta + \tfrac{b}{r}\sin\Theta\} \end{aligned} \tag{A9}$$

$$\begin{aligned} t_{gravity} = &\; mgr\cos\Theta + \\ &mr^2\dot{\Theta}^2\tan\Theta - \\ &\frac{(m_f + m)gr}{\cos\Theta} \end{aligned} \tag{A10}$$

$$\begin{aligned} t_{friction\_anterior} = &\; mgr\cos\Theta + \\ &[(m\sin\Theta + \cos\Theta)mr^2\dot{\Theta}^2 - \\ &mrg(m_f + m)]/[m\cos\Theta - \sin\Theta] \end{aligned} \tag{A11}$$

$$\begin{aligned} t_{friction\_posterior} = &\; mgr\cos\Theta + \\ &[(m\sin\Theta - \cos\Theta)mr^2\dot{\Theta}^2 - \\ &mrg(m_f + m)]/[m\cos\Theta + \sin\Theta] \end{aligned} \tag{A12}$$

We would like to acknowledge Dr. K. Iqbal for bringing this to our attention.